

Investigation of the Restricted Diffusion in Spherical Cavities of Polymers by Pulsed Field Gradient Nuclear Magnetic Resonance

Matthias Appel,* Gerald Fleischer, and Jörg Kärger

Fakultät für Physik und Geowissenschaften, Universität Leipzig,
Linnéstrasse 5, D-04103 Leipzig, Germany

A. C. Dieng and G. Riess

Ecole Nationale Supérieure de Chimie de Mulhouse, C.R.P.C.S.S.,
3 rue Alfred Werner, F-68093 Mulhouse, France

Received August 30, 1994; Revised Manuscript Received January 4, 1995[§]

ABSTRACT: We present results of pulsed field gradient nuclear magnetic resonance (PFG NMR) measurements of restricted diffusion of silicone oil (PDMS) dispersed in the continuous polystyrene phase of a two-phase system containing polystyrene (PS) and poly(dimethylsiloxane). These materials were synthesized by free-radical polymerization of styrene in a silicone oil/styrene emulsion in the presence of a polystyrene–poly(dimethylsiloxane) (PS–PDMS) block copolymer acting as an emulsifier. The diameters of the oil droplets could be derived from the echo attenuation plots of the PFG NMR experiments. They decrease with increasing temperature. The materials were observed to possess a thermally stable structure up to temperatures of 160 °C.

Introduction

Materials with self-lubricating properties are very interesting for technical applications. Polymers, especially poly(tetrafluoroethylene) and polyethylene, are widely used as solid lubricants for metallic surfaces. Self-lubricating properties can be caused either by the polymer structure itself or by inorganic or organic fillers incorporated into the polymer and decreasing the friction coefficient during sliding. A model for the latter system is a binary system of polystyrene (PS) and poly(dimethylsiloxane) (PDMS) with inclusions of poly(dimethylsiloxane) oil in the continuous polystyrene phase. The size of the silicone oil inclusions is regulated by means of a PS–PDMS diblock copolymer acting as an emulsifier. A layer of silicone oil is then present between the two rubbing materials producing the permanent lubricating properties of this system. Details of the synthesis and friction experiments for this special system investigated by us will be reported elsewhere.¹

An alternative approach for studying these substances is through the investigation of the self-diffusion of the included PDMS oil. Depending on the covered length scales, molecular transport may be very sensitive to the internal geometry of the sample. Therefore, molecular motion of the silicon oil within the droplets can be reliably identified by investigating the self-diffusion properties.

On the other hand, diffusion of molecules in closed cavities is a common process in nature, observable for a variety of systems including water in biological cells or oil in plants or sandstone.^{2,3} The self-lubricating polymers with inclusions of PDMS oil are well suited for these investigations, and, as reported in this paper, pulsed field gradient nuclear magnetic resonance (PFG NMR) measurements supply valuable data concerning the droplet sizes of the silicone oil in the PS matrix and their temperature dependence.

The determination of self-diffusion coefficients by means of PFG NMR spectroscopy is by now a standard

technique.^{4,5} It has been successfully applied in measuring diffusion within polymer melts and solutions^{6–8} or within microporous solids.^{9,10} Information about the structure of the investigated system can be derived from the time dependence of the NMR signal: for diffusion times shorter than the time needed by the diffusing particle for crossing the restricted geometry, most molecules experience free Brownian motion. On a time scale long compared to that needed to cover the distance between the boundaries, all molecules will have been repeatedly reflected at the walls. This causes the distribution of molecular displacements to be influenced by the length scales of the system rather than by molecular self-diffusion. This probe of the microstructure is known as “dynamical imaging”.⁵

It has already been shown that the magnetic field gradient NMR spin-echo experiment may be interpreted in terms of the generalized incoherent scattering function known from quasielastic neutron scattering (QENS).^{5,11} This concept includes a time-independent “elastic incoherent structure factor” (EISF) which contains information about the structure of the sample. PFG NMR can only be applied to this topic when the microscopic structure corresponds to the length scale probed by PFG NMR. This length scale is typically on the order of micrometers. So far, only a few PFG NMR experiments of this type have been performed. The polymer system investigated by us with included oil droplets may be considered as a model substance for the interpretation of PFG NMR spin-echo experiments in terms of the generalized incoherent scattering function.

In this paper, we report results of PFG NMR measurements of restricted self-diffusion of the PDMS oil within spherical cavities over a broad temperature range. We have extracted information from NMR experiments regarding the structure and the thermal behavior of the polymer.

In the first part of this paper we summarize the theoretical background of these experiments. In the experimental section, we describe the investigated samples and the results of our measurements. Finally,

* To whom correspondence should be addressed.

[§] Abstract published in *Advance ACS Abstracts*, March 1, 1995.

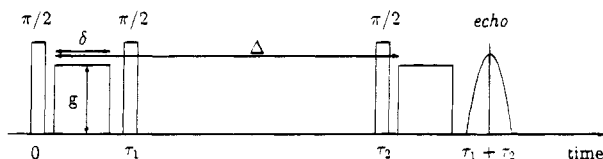


Figure 1. Stimulated echo sequence for pulsed field gradient self-diffusion measurements. Magnetic field gradients of strength g and duration δ are applied both in the evolution period and in the detection period. The diffusion time t is equal to the time Δ between the two field gradient pulses if $\delta \ll \Delta$.

we summarize and discuss the results of this investigation.

PFG NMR

Field gradient NMR is based on the ability to produce a spatial dependence of the Larmor frequency $\omega(\vec{r})$ of a spin by application of a magnetic field gradient \vec{g} in addition to the constant magnetic field B_0

$$\omega(\vec{r}) = \gamma B_0 + \gamma \vec{g} \cdot \vec{r} \quad (1)$$

with γ denoting the gyromagnetic ratio of the spins under study.

For the determination of the self-diffusion coefficients of the investigated samples, we used the stimulated echo sequence. The pulse program of this technique is given in Figure 1. The stimulated echo sequence has the advantage of allowing the use of large times Δ between the two field gradient pulses if the longitudinal relaxation time T_1 is much longer than the transverse relaxation time T_2 . In polymers this is most often the case.

The NMR signal at time $\tau_1 + \tau_2$ (the "stimulated" echo) results as a superposition of transverse magnetizations. Neglecting the influences of longitudinal and transverse relaxation, the signal intensity attenuation ψ is determined by (1) the probability density that a particle is initially (i.e., during the first gradient pulse) situated at position \vec{r}_0 , which under equilibrium condition is equal to the particle density $\varrho(\vec{r}_0)$, (2) the probability density that a particle can be found at the position $\vec{r} = \vec{r}_0 + \vec{R}$ at time t (instant of the second gradient pulse) if it has been at position \vec{r}_0 at time 0 (instant of the first gradient pulse) [this conditional probability is described by the "propagator" $P_S(\vec{r}_0|\vec{r}, t)$], and (3) the influence of the magnetic field gradients producing a resulting phase shift $\Delta\phi = \gamma \delta \vec{g} \cdot \vec{R}$.

The signal intensity (echo) attenuation due to diffusion may be shown to be given by

$$\psi(\vec{q}, t) \int \int \varrho(\vec{r}_0) P_S(\vec{r}_0|\vec{r}_0 + \vec{R}, t) \exp(i\vec{q} \cdot \vec{R}) d\vec{R} d\vec{r}_0 \quad (2)$$

where the quantity

$$\vec{q} = \gamma \delta \vec{g} \quad (3)$$

is a generalized scattering vector. The space scale scanned by the stimulated echo experiment is equal to the reciprocal scattering vector $1/q$.

Equation 2 may be transferred into

$$\psi(\vec{q}, t) = \int P_S(\vec{R}, t) \exp(i\vec{q} \cdot \vec{R}) d\vec{R} \quad (4)$$

by introducing an "averaged" propagator¹²

$$P_S(\vec{R}, t) = \int \varrho(\vec{r}_0) P_S(\vec{r}_0|\vec{r}_0 + \vec{R}, t) d\vec{r}_0 \quad (5)$$

Equation 4 coincides with the intermediate incoherent scattering function $S_{inc}(\vec{q}, t)$, with the only difference that, following van Hove's pioneering paper,¹³ the above-introduced mean propagator is generally called the self-correlation function and denoted by $G_S(\vec{R}, t)$. PFG NMR data may therefore be easily interpreted in terms of the formalism derived for the interpretation of QENS data. Following this procedure, we split the mean propagator into a time-independent part $P_S(\vec{R}, \infty)$ and a part decaying to zero for long diffusion times, $P'_S(\vec{R}, t)$.

$$P_S(\vec{R}, t) = P_S(\vec{R}, \infty) + P'_S(\vec{R}, t) \quad (6)$$

Using equations 4 and 6, one thus obtains

$$\psi(\vec{q}, t) = \int P'_S(\vec{R}, t) \exp(i\vec{q} \cdot \vec{R}) d\vec{R} + \int P_S(\vec{R}, \infty) \exp(i\vec{q} \cdot \vec{R}) d\vec{R} \quad (7)$$

That means the echo attenuation is found to consist of a time-dependent term (the first one on the right-hand side of equation 7) and a time-independent term. This second term corresponds to the EISF known from neutron scattering. It contains information regarding the space that can be reached by a tagged particle during the experiment.

In systems with restricted diffusion, there exists a distinct time τ_c , in which the species have moved a length comparable with the distance d between the boundaries.

$$\tau_c \approx d^2/D \quad (8)$$

For diffusion times shorter than τ_c , most molecules carry out free Brownian motion represented by the self-diffusion coefficient D_S . The propagator is Gaussian and the NMR signal $\psi(\vec{q}, t)$ for short diffusion times can be calculated to be

$$\psi(\vec{q}, t) = \exp(-q^2 D t) \quad (9)$$

On a time scale long compared with τ_c , all molecules will have been reflected at the walls many times. The propagator, therefore, simplifies to the probability of finding a molecule anywhere between the boundaries. In this case, the probability density $P_S(\vec{r}_0|\vec{r}_0 + \vec{R}, t)$ is identical to the molecular density function $\varrho(\vec{r})$.

For the NMR signal attenuation in the long-time limit, one obtains from eq 2 after a few steps

$$\psi(\vec{q}, \infty) = |I(\vec{q})|^2 \quad (10)$$

with $I(\vec{q})$ denoting the Fourier transform of the density function $\varrho(\vec{r})$

$$I(\vec{q}) = \int \varrho(\vec{r}) \exp(-i\vec{q} \cdot \vec{r}) d\vec{r} \quad (11)$$

Equation 10 provides a straightforward means to calculate the long-time limit of the NMR signal attenuation in the case of restricted diffusion. It is the basis for determining structural information from PFG NMR, known as "dynamical imaging".⁵

For spherical cavities one obtains

$$\psi(q, \infty) = \frac{9(qa \cos(qa) - \sin(qa))^2}{(qa)^6} \quad (12)$$

For sufficiently small values of qa , equation 12 can be approximated by

$$\psi(q, \infty) = \exp(-q^2 a^2/5) \quad (13)$$

In this case, a comparison with the standard relation for unrestricted diffusion (eq 9) would yield an apparent, time-dependent, self-diffusion coefficient, determined by the relation

$$D_{\text{app}} = a^2/5t \quad (14)$$

This approximation holds up to qa values of about 2.⁵

The characteristics of the attenuation of the NMR signal in the case of restricted diffusion in spherical cavities may be summarized as follows: (i) For short diffusion times, the molecules diffuse freely with a self-diffusion coefficient D_S . The echo attenuation is given by eq 9. (ii) In the long-time limit the NMR signal is independent of the diffusion time (eq 12) and coincides with the EISF introduced in QENS. This EISF is only determined by the boundary distances. The crossover from free to restricted diffusion occurs at

$$t_C = a^2/5D_S \quad (15)$$

with a denoting the radius of the spherical cavities.

Experimental Part

The investigated samples were binary systems of polystyrene and poly(dimethylsiloxane) with inclusions of PDMS oil in the continuous polystyrene phase. The materials were obtained by polymerization of styrene in silicone oil (PDMS)/styrene emulsions in the presence of a polystyrene-poly(dimethylsiloxane) (PS-PDMS) block copolymer acting as an emulsifier.

The PS-PDMS block copolymer was prepared by sequential anionic polymerization of styrene and cyclic hexamethyltrisiloxane (D3) in a tetrahydrofuran solution, using *sec*-butyllithium as an initiator.

The details of the preparation and purification techniques have been given elsewhere.¹ The purified copolymer is characterized by GPC and ¹H NMR. The average molecular weight (M_n) of the copolymer is 50 500 and its PDMS content 17 wt %.

The two-phase systems are obtained by dispersion of a liquid (PDMS oil 1000 from Rhone-Poulenc) in a PS matrix. An emulsion of PDMS oil in styrene is prepared by stirring a mixture of styrene, block copolymer (5 wt % with respect to the styrene phase), and PDMS oil (10–40 wt %). At first, 10 wt % (with respect to the styrene phase) PS homopolymer is dissolved in styrene to favor the stability of the emulsion. The stable emulsion is polymerized by adding 1 wt % (with respect to the styrene phase) of benzoyl peroxide.

When the oil content is above 20 wt %, 5 wt % of divinylbenzene (DVB) as a cross-linking agent is added to the emulsion. Semi-IPN systems were then formed.

The compositions of the prepared materials are given in Table 1.

Figure 2 represents SEM pictures of the morphology of two samples containing 20 wt % oil. The upper one is prepared with 5 wt % of copolymer (sample 2) and the lower one with 10 wt % of copolymer (sample 4). The diameters of the oil droplets are reduced when the copolymer content is increased.

The diffusion measurements have been carried out by means of the PFG NMR spectrometer FEGRIS 60⁴ using a proton resonance frequency of 60 MHz. Due to the very long nuclear

Table 1. Composition of the Prepared and Investigated Samples

sample	total PS content (wt %)	copolymer content (wt %) ^b	total PDMS content (wt %) ^c
1	89.2	5	10.8
2	79.3	5	20.7
3	55.5 ^a	5	40.5
4	71.2	10	21.4

^a Semi-IPN system. ^b With respect to the styrene phase. ^c Silicone oil + PDMS from the copolymer.

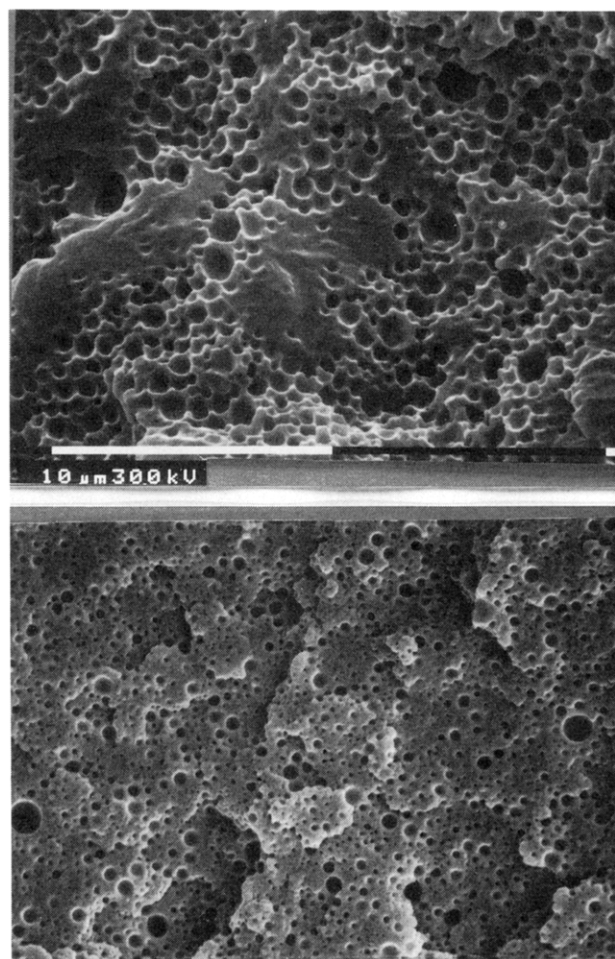


Figure 2. SEM pictures of the morphology of PS-PDMS composites with 20 wt % silicone oil: (a, top) sample 2; (b, bottom) sample 4.

magnetic relaxation times of the PDMS, the diffusion time t could be varied between a few milliseconds and about 2 s. The magnitude of the scattering vector \vec{q} was increased by varying both the length δ and the intensity g of the field gradient pulses. In our experiments, g values up to 11.7 T/m were applied. The temperature was varied between room temperature and 160 °C.

Results and Discussion

Figure 3 shows the dependence of the echo attenuation ψ on the diffusion time t for different scattering vectors q for the sample 2 with 20% oil inclusions, from room temperature up to 160 °C. For all temperatures the echo attenuation was found to attain a constant value for sufficiently large observation times. Similar results were obtained with sample 4. One has to conclude, therefore, that all molecules contributing to the observed NMR signal are contained in confined spaces, which are clearly to be identified with the droplets of PDMS oil. The droplets of the oil inclusions

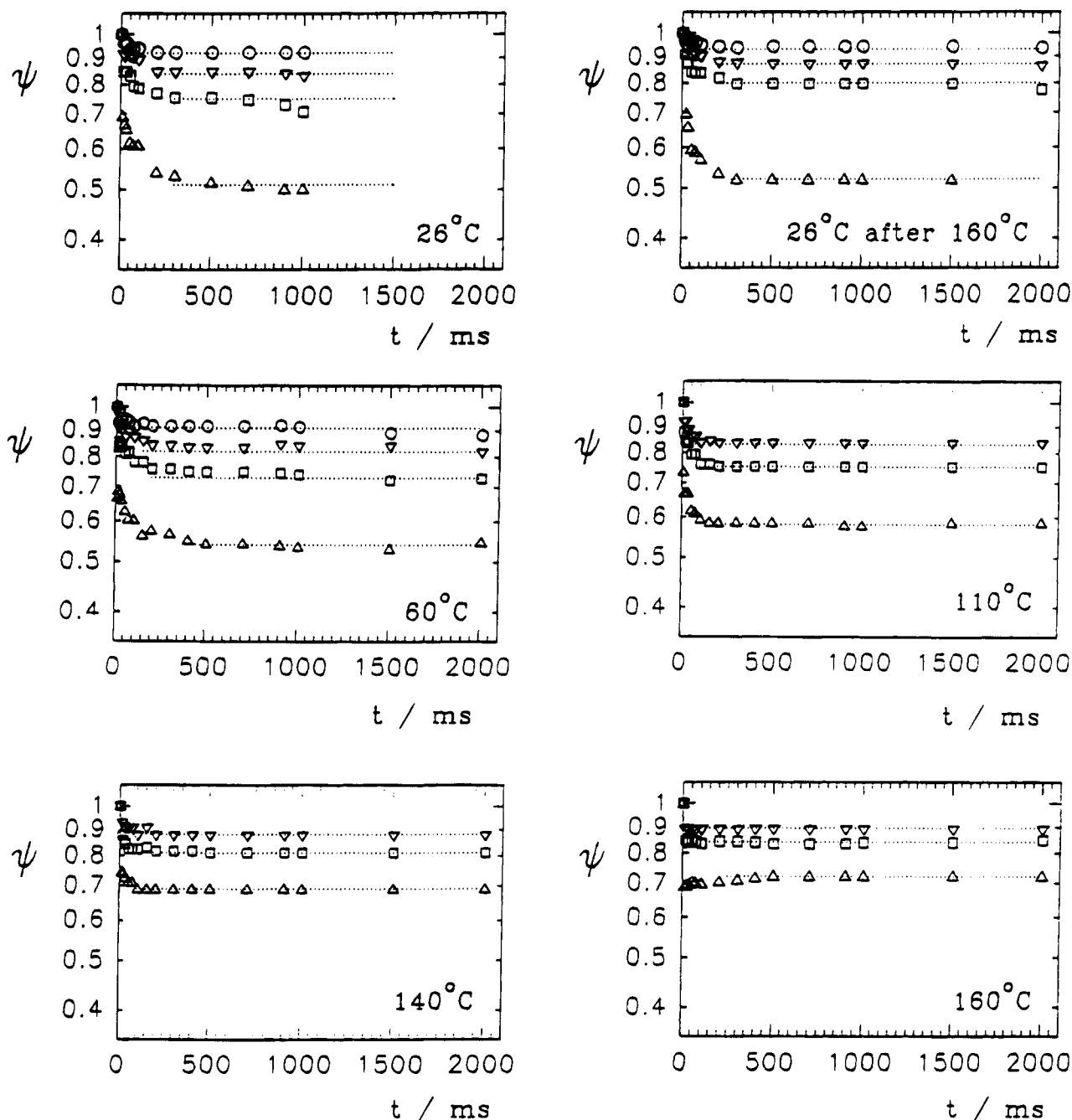


Figure 3. Echo attenuation plots for sample 2 with 20% oil inclusions between 26 and 160 °C. The applied q values are 1.13×10^6 (○), 1.71×10^6 (▽), 2.27×10^6 (□) and 3.41×10^6 m⁻¹ (△).

in sample 1 are of such size that only for the highest temperature a time-independent EISF could be observed. Therefore, the droplets may be estimated to be larger than about 1.2 μm .

According to eq 13, there should be an exponential relation between the time-independent part of the spin-echo attenuation and q^2 . Figure 4a demonstrates that this prediction is in excellent agreement with the behavior observed experimentally.

By application of eq 13, the radius a of the spherical cavities can be calculated from the slope of these curves. The results are shown in Figure 4b for samples 2 and 4. The droplet radii are in agreement with the SEM pictures of Figure 2. Here it must be mentioned that we have disregarded any polydispersity of the droplet sizes in our data evaluation. This polydispersity is, of course, present in the samples, as may be seen in Figure

2. If the size distribution is known or if reasonable assumptions are possible, the distribution can be taken into account, and from very precise measurements of $\psi(q)$, a correct average of the radii can be evaluated.² The size distribution of our radii is unknown; however, it can be stated that the larger droplets in the sample are stronger weighted. The polydispersity effects in our samples are not very pronounced; otherwise, the echo attenuation at the crossover from free to restricted diffusion around τ_c would be considerably broadened.

Figure 4b reveals the remarkable result that the radii of the droplets decrease with increasing temperature. This can only result from the solubility of the PDMS oil in the matrix which increases with increasing temperature. Therefore, the amount of PDMS oil in the droplets decreases.

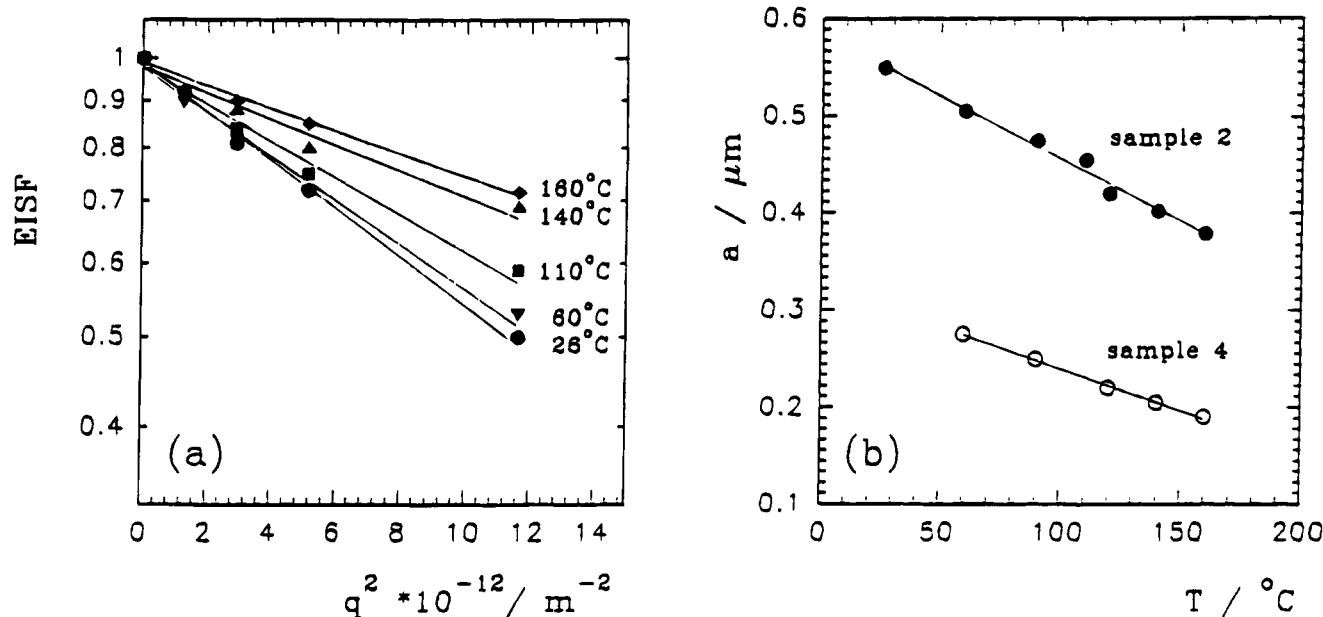


Figure 4. (a) q^2 dependence of the EISF at several temperatures for sample 2 and (b) the temperature dependence of the droplet radii derived from the EISF according to eq 13 for samples 2 and 4, both having a 20% oil content but differing in their amount of PS-PDMS copolymer. The straight lines are only guides for the eye.

Due to the lower mobility in the rigid matrix, the proton nuclear magnetic relaxation times of the dissolved oil molecules are so short that the signal is exclusively due to the molecules within the droplets; i.e., the oil molecules dissolved in the matrix are invisible at our experimental time scale. Therefore, we are not able to detect the diffusion of the silicone oil dissolved in the PS matrix immediately. However, the permeability of the oil through the matrix from one droplet to a neighboring one must result in a slow long-time diffusivity in our experiment. In Figure 3 we do not observe any decrease of $\psi(t)$ for long diffusion times t within experimental accuracy. The long-time diffusivity must be, therefore, smaller than $10^{-15} \text{ m}^2/\text{s}$ if present at all. It has been ascertained by analyzing high-resolution NMR spectra that with increasing temperature the amount of oil molecules dissolved in the solid matrix is in fact increasing. A quantitative analysis of this correlation is the subject of future investigations.

A higher concentration of diffusant in a structured rubbery matrix allows the measurement of the self-diffusion in dependence of the diffusion time¹⁴ which provides valuable information about structure and mobility in the system. Unfortunately, these experiments are not possible with our system.

A careful inspection of Figure 4b indicates a stronger drop of the droplet radius if the glass transition temperature of polystyrene ($\approx 100^\circ\text{C}$) is crossed and the solubility of PDMS oil in the PS matrix increases. Due to this swelling of the matrix, the surface and form of the droplets get more and more distorted, resulting in an additional restriction of the oil diffusion. As it can be seen in Figure 4a, the $\psi(q, \infty)$ dependence according to eq 13 becomes more and more nonexponential with increasing temperature, indicating deviations from eq 13 and its underlying assumptions. At high temperatures the droplet radius determined from Figure 4a with eq 13 should only be considered as a geometric measure of the effective droplet volume. Nevertheless, the samples have a remarkable thermal stability though the matrix of samples 2 and 4 is not cross-linked. The thermal behavior is reversible; i.e., the original droplet

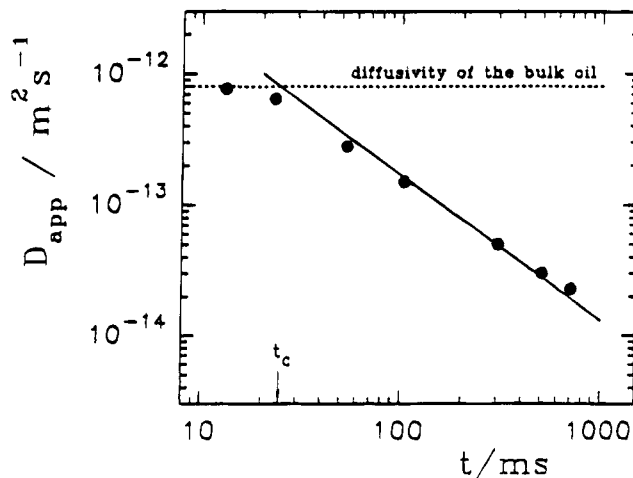


Figure 5. Apparent diffusion coefficient D_{app} according to eq 14 as a function of diffusion time t for sample 4 with 20% dispersed silicone oil at room temperature. For times longer than the crossover time t_c the diffusion coefficient scales with t^{-1} .

radii are again reached after cooling the sample down from 160°C to room temperature.

Figure 5 reflects the PFG NMR diffusivity data for sample 4 with 20% dispersed silicone oil at room temperature in terms of an apparent diffusivity. This representation is based on the application of eq 9 to analyze the PFG NMR experiments. For sufficiently short observation times ($t < t_c$) the measured diffusivity coincides with the value for unrestricted diffusion, while for sufficiently large observation times the apparent diffusivity is exclusively determined by the size of the confinements as predicted by eq 14, being proportional to the reciprocal of the observation time. The calculated (eq 15) and observed values for t_c agree very well.

Figure 6a shows the echo attenuation observed for sample 3 with 40% oil inclusions. In striking contrast to the behavior of the polymers with smaller oil content (cf. Figure 3), the spin-echo amplitude is found to decay monotonously with increasing observation time, without approaching a constant value. Hence, no EISF is

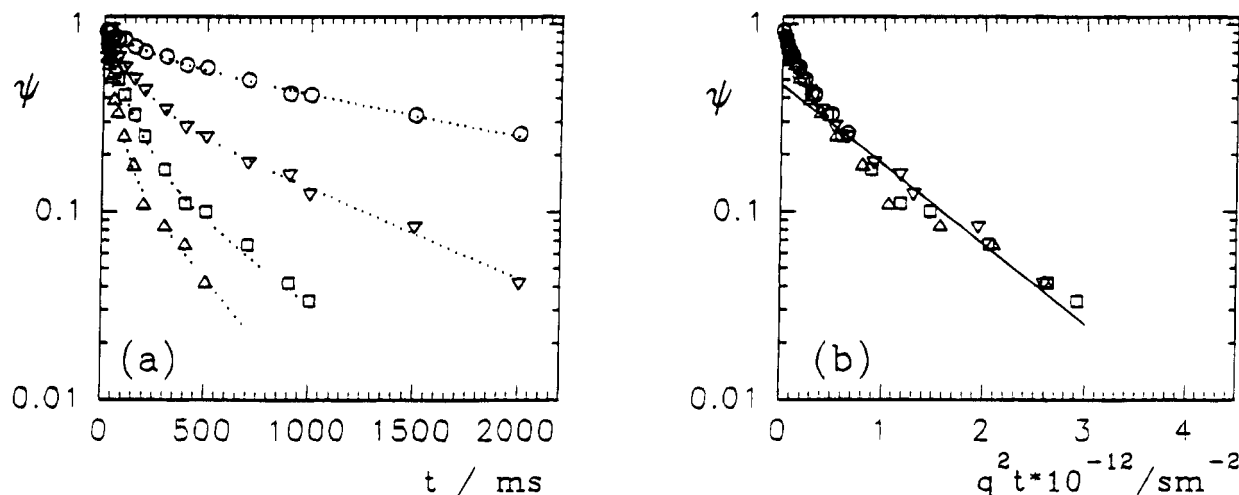


Figure 6. Echo attenuation plots for a sample with 40% oil inclusions at 110 °C: (a) the NMR signal as a function of only the diffusion time; (b) the echo attenuation versus q^2t as a master plot ($q = 0.56 \times 10^6$ (○), 1.14×10^6 (▽), 1.70×10^6 (□), and 2.31×10^6 m $^{-1}$ (△)). From the slope of the exponentially decaying part, the self-diffusivity of the bulk oil phase is equal to 1.3×10^{-12} m 2 /s.

observed. One has to conclude, therefore, that during the accessible observation times the diffusing molecules are not subjected to any confinement; the droplets are too large and hence beyond the space window of our experiments. It is demonstrated by the representation of Figure 6b that the echo attenuation is a sole function of q^2t . We observe free diffusion of the oil, and eq 9 representing the case of unrestricted diffusion is valid. The observed deviation from a single-exponential dependence must be attributed to the polydispersity of the silicone oil. From the slope of the straight line in Figure 6b, the self-diffusivity of the oil via eq 9 is equal to 1.3×10^{-12} m 2 /s at 110 °C. If there were any crossover from free to restricted diffusion, it must occur for observation times much larger than the maximum observation time ($t_{\max} = 2$ s) realized in the present experiments. Inserting this value into eq 14, the radius of molecular confinements in the 40% sample may be estimated to be larger than 3.5 μ m.

Summary and Conclusions

We have synthesized and investigated by PFG NMR binary polymer systems consisting of PDMS oil dispersed in a polystyrene matrix. As an example of "dynamic NMR imaging", PFG NMR was applied for studying the droplet radii, their temperature dependence, and the translational mobility of the PDMS oil. The droplet radius a can be evaluated from the PFG NMR experiment if an EISF is observed. This can be realized if the condition $qa \approx 1$ is fulfilled. For two of the four samples the droplet radii could be determined. They are in good agreement with SEM pictures. With increasing temperature, the radii determined by PFG NMR decrease. This is caused by swelling of the matrix connected with a loss of oil from the droplets. For higher temperatures above the glass transition temperature of the polystyrene matrix a deformation of the form and the surface of the cavities may additionally

restrict the diffusion of the oil. We could not observe any permeation of the oil through the PS matrix. The investigated binary polymer systems are thermally stable up to 160 °C; i.e., on heating to 160 °C and thereafter cooling down to room temperature, the PFG NMR echo attenuations are completely reproducible.

Acknowledgment. The authors thank L. Lavielle, Centre de Recherches sur la Physico-Chimie, France, for her interest in this work. We are grateful to W. Heink from our department for technical assistance. Financial support of the Deutsche Forschungsgemeinschaft (SFB 294) is greatly appreciated.

References and Notes

- (1) Dieng, A. C.; Riess, G.; Lavielle, L.; Brendle, M. *New Polym. Mater.*, submitted for publication.
- (2) Fleischer, G.; Skirda, V. D.; Werner, A. *Eur. Biophys. J.* **1990**, *19*, 25.
- (3) Sen, P. N.; Schwartz, L. M.; Mitra, P. P. *Magn. Reson. Imaging* **1994**, *12*, 227.
- (4) Kärger, J.; Pfeifer, H.; Heink, W. *Adv. Magn. Reson.* **1988**, *12*, 1.
- (5) Callaghan, P. T. *Principles of Nuclear Magnetic Resonance Microscopy*; Clarendon Press: Oxford, U.K., 1991.
- (6) Appel, M.; Fleischer, G.; Kärger, J.; Fujara, F.; Chang, I. *Macromolecules* **1994**, *27*, 4274.
- (7) Appel, M.; Fleischer, G. *Macromolecules* **1993**, *26*, 5520.
- (8) Fleischer, G.; Zgadzai, D. E.; Skirda, V. D.; Maklakov, A. I. *Colloid Polym. Sci.* **1988**, *266*, 201.
- (9) Kärger, J.; Ruthven, D. M. *Diffusion in Zeolites and Other Microporous Solids*; Wiley: New York, 1992.
- (10) Pfeifer, H. In *NMR—Basic Principles and Progress*; Kosfeld, R., Blümich, B., Eds.; Springer-Verlag: Berlin, Heidelberg, New York, 1994; Vol. 31, p 31.
- (11) Fleischer, G.; Fujara, F. In *NMR—Basic Principles and Progress*; Kosfeld, R., Blümich, B., Eds.; Springer-Verlag: Berlin, Heidelberg, New York, 1994; Vol. 30, p 161.
- (12) Kärger, J.; Heink, W. *J. Magn. Reson.* **1983**, *51*, 1.
- (13) van Hove, L. *Phys. Rev.* **1954**, *95*, 249.
- (14) von Meerwall, E.; Shook, D.; Min, K. J.; Kelley, F. N. *J. Appl. Phys.* **1984**, *56*, 2444.

MA945058A